Electron scattering by spatially correlated DX charges

C. Ghezzi and A. Parisini
Dipartimento di Fisica, Università di Parma, Viale delle Scienze, 43100 Parma, Italy

V. Dallacasa
Dipartimento di Fisica, Università di Udine, Viale delle Scienze 33100 Udine, Italy
(Received 1 February 1994)

Electron scattering by a spatially correlated system of DX charges has been described using the formalism of composition waves. The matrix element for the scattering rate is given through an $I(\vec{Q})$ interference function ($\vec{Q}$=scattering vector) containing pair correlation functions $\epsilon(\vec{\rho})$ defined at the $\vec{\rho}$ lattice vectors. The $\epsilon(\vec{\rho})$ are able to describe long-range as well as short-range order and they are simply related to short-range order correlation functions given in the literature. The method is developed for scattering centers having equal charges; the case of positively and negatively charged impurities present together is briefly discussed. A comparison between the two extreme cases of randomly distributed scattering centers and of centers arranged in a superlattice suggests, for intermediate cases, an $I(\vec{Q})$ given by an array of Gaussian shaped functions with common dispersion σ, centered on the reciprocal nodes of a virtual superlattice. On this basis, experimental mobility data for Si-doped $Al_{0.25}Ga_{0.75}As$ samples prepared by molecular beam epitaxy have been analyzed and discussed. Data refer to isothermal electron capture transients into DX centers, as well as to steady-state measurements taken for different free electron densities under a persistent photoconductivity regime. It has been confirmed that the initial stage of the capture process takes place together with increasing order in the scattering center distribution (decreasing σ), whereas the contrary happens during the final stage (increasing σ).

I. INTRODUCTION

The importance of interimpurity interactions in affecting the low-temperature electron mobility in heavily n-doped semiconductors is widely recognized. When the empty donors begin to capture electrons, there is the possibility for the electron charges to be redistributed among the randomly distributed donors in such a way that the total electrostatic energy is minimized. Because of the partial occupation, the interdonor Coulomb interaction causes the formation of a spatially correlated system of donor charges. As a consequence of this partial ordering, a mobility higher than the expected one for a system of randomly distributed impurity charges can then be observed under conditions where impurity scattering dominates.

DX centers in n-type $Al_xGa_{1-x}As$ (Refs. 1 and 2) constitute a charged impurity system which is particularly attractive from the above point of view. It is now generally accepted that the DX center is due to the isolated donor impurity. Moreover, a number of experimental results can be more easily explained by assuming that the isolated donor has a bistable behavior between the ordinary substitutional configuration and a lattice-distorted one, the DX center being the ground state of the distorted configuration. There is also a growing consensus to the idea that the distorted configuration is stabilized by the capture of two electrons by the center, this latter having thus a negative DX^- charge state and a negative Hubbard correlation energy U. Anyway, the main practical advantage of DX center systems is that, owing to the well known persistent photoconductivity effect taking place at low temperature, the fraction of empty donors can be easily adjusted to any desired level at the same temperature.

The significance of spatial correlations among DX charges has recently been pointed out in a number of studies, performed under diverse experimental conditions. O'Reilly[3] and Kossut *et al.*[4] suggested that such correlations should be accounted for in order to explain the increase in low-temperature mobility, observed in GaAs subject to hydrostatic pressure.[5,6] By varying the hydrostatic pressure at low temperature, Suski *et al.*[7] were able to separate the modifications of the mobility due to alterations in the band structure of GaAs from those related to correlations among DX charges. Wilamowski *et al.*[8] demonstrated that such correlations are destroyed by the photoionization process of the DX centers. Piotrzkowski *et al.*[9] produced different DX center configurations using a combined effect of pressure, illumination and temperature in a $Al_xGa_{1-x}As$ alloy ($x = 0.15$), and they observed different $\mu = \mu(n)$ curves (μ = mobility, n = electron density) upon warming the sample, depending on the configuration. Jantsch *et al.*[10] observed hysteresis in the time resolved mobility $\mu = \mu(n)$ diagram obtained above 100 K by increasing n with illumination and by decreasing n through capture. Finally, Coz *et al.*[11] demonstrated that the low-temperature electron mobility in Si-doped $Al_{0.25}Ga_{0.75}As$ is not a single valued function of n, μ being larger if a given n value is reached through capture rather than photoionization processes.

Spatial correlations of donor charges have been described using different approaches. O'Reilly[3] argued that

the initial formation of DX^- centers involves replacing close pairs of positive charges by dipoles. The variations in mobility due to carrier trapping is then determined by the corresponding reduction in the scattering cross section. Wilamowski *et al.*[12] used the model of impurity self-screening. An effective Thomas-Fermi screening radius is evaluated which includes the screening by the impurities themselves in addition to free electron screening. The former has to be evaluated in a self-consistent way from the energy distribution of impurity states. A quantitative interpretation of mobility data is very complicated, however, owing to the need to accounting for the self-screening of the four *DX* states arising from different numbers of Al next to neighbor atoms around the donor. These complications are avoided if a different approach is introduced, based on the use of pair correlation functions $g(r)$ to describe the short-range order configurations around the impurities.[4,7,8,13] In this way the scattering cross section can be evaluated as a function of the $\vec{Q}$ scattering vector by multiplying the scattering amplitude of the isolated impurity with an appropriate structure factor $S(Q)$.

In this work, the spatial distribution of charged impurities is described using the formalism of composition waves, as earlier introduced to analyze coherent x-ray or neutron scattering in solid solutions.[14,15] A brief outline of the method has already been given in Ref. 16. Using the first Born approximation, the matrix element for the scattering rate is given through an interference function $I(\vec{Q})$ containing pair correlation functions $\epsilon(\vec{\rho})$ defined at the $\vec{\rho}$ lattice vectors. The $\epsilon(\vec{\rho})$ are able to describe long-range as well as short-range order and they are simply related to the above mentioned $g(r)$. In Sec. II the method is developed for the case when only positively charged donors are present. In Sec. III the case of positively and negatively charged impurities present together is briefly discussed. A comparison between the two extreme cases of randomly distributed scattering centers and of centers arranged in a superlattice suggests, for intermediate cases, a $I(\vec{Q})$ given by an array of gaussian shaped functions centered on the reciprocal nodes of a virtual superlattice. On this basis, an analysis of experimental mobility data of Si-doped $Al_xGa_{(1-x)}As$ is given in Sec. IV.

II. POSITIVELY CHARGED CENTERS

A. Outline of the method

Consider an n-type semiconductor. For the sake of simplicity, let us neglect acceptors and assume a positive Hubbard correlation energy U for the donor impurities. In this way, the scattering centers are the positively charged donors D^+, whose number will be indicated by $N(D^+)$. Their spatial distribution can be described as follows. For each $\vec{l}$ vector of the space lattice (diamond-like semiconductors have a fcc space lattice) let us define a variable $\xi(\vec{l})$ which is equal to 1 if the proper site of the $\vec{l}$th primitive cell is occupied by a D^+, $\xi(\vec{l}) = 0$ otherwise. The scattering potential for the electron is then

$$U(\vec{r}) = \sum_{\vec{l}} U_i(\vec{r} - \vec{l})\xi(\vec{l}), \tag{1}$$

where $U_i(\vec{r} - \vec{l})$ means the potential due to an isolated D^+ in $\vec{l}$. Free electron screening is included in U_i. Being defined at space lattice nodes, $\xi(\vec{l})$ can be written as a superposition of N (N = number of primitive cells) composition waves, having wavevectors $\vec{q}$ and amplitudes $\xi(\vec{q})$, as

$$\xi(\vec{l}) = \sum_{\vec{q}} \xi(\vec{q}) \exp(-i\vec{q} \cdot \vec{l}). \tag{2}$$

Using the first Born approximation, the matrix element for the transition rate from a plane wave state $\vec{k}$ to $\vec{k}'$ is then

$$| \langle \vec{k} | U(\vec{r}) | \vec{k}' \rangle |^2 = N^2 | f_i(\vec{Q}) |^2 | \xi(\vec{Q}) |^2 \qquad (\vec{Q} = \vec{k} - \vec{k}'). \tag{3}$$

Here $\vec{Q}$ is the scattering vector, $f_i(\vec{Q})$ given by

$$f_i(\vec{Q}) = \int U_i(\vec{r} - \vec{l}) \exp\left[i\vec{Q} \cdot (\vec{r} - \vec{l})\right] d\vec{r} \tag{4}$$

is the scattering amplitude for the isolated impurity, and

$$| \xi(\vec{Q}) |^2 = \frac{1}{N^2}\left(\sum_{\vec{l}} \xi^2(\vec{l}) + \sum_{\vec{l},\vec{l}'}^{\vec{l}\neq\vec{l}'} \xi(\vec{l})\xi(\vec{l}') \exp[i\vec{Q} \cdot (\vec{l} - \vec{l}')]\right). \tag{5}$$

This last quantity is more usefully replaced by its ensemble average

$$\langle | \xi(\vec{Q}) |^2 \rangle = \frac{1}{N}\left(\xi + \sum_{\vec{\rho}\neq 0} \epsilon(\vec{\rho}) \exp(i\vec{Q} \cdot \vec{\rho})\right), \tag{6}$$

where $\xi = N(D^+)/N$ is the mean value of $\xi(\vec{l})$ over a macroscopic portion of the crystal and

$$\epsilon(\vec{\rho}) \equiv \langle \xi(\vec{l})\xi(\vec{l}') \rangle_{\vec{\rho}=\vec{l}-\vec{l}'} \tag{7}$$

means the average of the product $\xi(\vec{l})\xi(\vec{l}')$ over all pairs separated by the $\vec{\rho} = \vec{l} - \vec{l}'$ lattice vector.

The scattering probability can then be evaluated as a function of the state of order of the D^+ distribution, this latter being described by the pair correlation parameters $\epsilon(\vec{\rho})$. The function

$$I(\vec{Q}) = \frac{N}{\xi}\langle | \xi(\vec{Q}) |^2 \rangle = 1 + \xi^{-1} \sum_{\vec{\rho}\neq 0} \epsilon(\vec{\rho}) \exp(i\vec{Q} \cdot \vec{\rho}) \tag{8}$$

can now be introduced, so that the matrix element is

$$|\langle \vec{k} \mid U(\vec{r}) \mid \vec{k}' \rangle|^2 = N(D^+) \mid f_i(\vec{Q}) \mid^2 I(\vec{Q}), \tag{9}$$

that is $I(\vec{Q})$ times the one for $N(D^+)$ independent, isolated charged donors. We shall denominate $I(\vec{Q})$ the interference function. The shape of $I(\vec{Q})$ is clearly dependent on the spatial distribution of the D^+ charged donors, whereas its integral over the Brillouin zone (BZ) is not. In fact, $I(\vec{Q})$ satisfies the sum rule

$$\sum_{\vec{Q}}^{\mathrm{BZ}} I(\vec{Q}) = N \tag{10}$$

as can be easily demonstrated from Eq. (8).

B. The interference function

Let us now consider two extreme cases: (i) an ideally random D^+ distribution and (ii) a superlattice arrangement of the D^+ charged donors.

In an ideally random distribution [case (i)]

$$\epsilon(\vec{\rho}) = \langle \xi(\vec{l})\xi(\vec{l}') \rangle_{\vec{\rho}} = \langle \xi(\vec{l}) \rangle \langle \xi(\vec{l}') \rangle = \xi^2 \tag{11}$$

is independent of $\vec{\rho}$, so that

$$|\langle \vec{k} \mid U(\vec{r}) \mid \vec{k}' \rangle|^2$$

$$= N \mid f_i(\vec{Q}) \mid^2 \left(\xi(1-\xi) + \xi^2 \sum_{\vec{\rho}} \exp(i\vec{Q} \cdot \vec{\rho}) \right). \tag{12}$$

Here the first term represents the "von Laue" diffuse scattering, which is characteristic of the random nature of the distribution. The last term, being vanishing unless $\vec{Q}$ coincides with a reciprocal lattice vector, represents Bragg scattering by a virtual crystal of charged impurities having scattering amplitude $\xi f_i(\vec{Q})$.

Avoiding Bragg scattering the interference function is

$$I(\vec{Q}) = (1-\xi) \qquad (\text{for } \vec{Q} \neq 0) \tag{13}$$

and

$$I(\vec{Q}) = (1-\xi) + N\xi \qquad (\text{for } \vec{Q} = 0). \tag{14}$$

The sum rule (10) is easily verified, since

$$\sum_{\vec{Q}}^{\mathrm{BZ}} I(\vec{Q}) = (1-\xi)(N-1) + (1-\xi) + N\xi = N. \tag{15}$$

In the cases in point, $N(D^+)$ is much smaller than the N available sites, so that $\xi \ll 1$ and $I(\vec{Q}) \approx 1$. Owing to Eq. (9), the system of $N(D^+)$ randomly distributed charged donors behaves as $N(D^+)$ independent, isolated scattering centers. However, the case $\xi = 1$ represents a regular array of charged impurities occupying all the available lattice sites. In this case the von Laue term vanishes and only Bragg scattering remains in Eq. (12), as expected.

The opposite extreme situation [case (ii)] is characterized by a superlattice arrangement of the D^+ charged donors. The superlattice will be defined by a system of $N(D^+)$ vectors $\vec{s}$, a subsystem of the fcc lattice vectors $\vec{l}$. All the $\vec{s}$ sites are occupied by D^+, any different lattice site $\vec{l} \neq \vec{s}$ being empty or occupied by a neutral donor D^o. Thus

$$\xi(\vec{l})\xi(\vec{l}')_{\vec{\rho}} = \delta_{\vec{\rho},\vec{s}} \qquad (\vec{\rho} = \vec{l} - \vec{l}'), \tag{16}$$

where δ is the Kronecker symbol. From Eq. (5) we get

$$\mid \xi(\vec{Q}) \mid^2 = \frac{1}{N^2} \left(N(D^+) + N(D^+) \sum_{\vec{s} \neq 0} \exp(i\vec{Q} \cdot \vec{s}) \right)$$

$$= \frac{\xi}{N} \sum_{\vec{s}} \exp(i\vec{Q} \cdot \vec{s}). \tag{17}$$

Equation (17) represents Bragg scattering by the superlattice, the summation over $\vec{s}$ being vanishing unless $\vec{Q}$ coincides with a $\vec{g}_s$ reciprocal superlattice vector.

The interference function

$$I(\vec{Q}) = \sum_{\vec{s}} \exp(i\vec{Q} \cdot \vec{s}) \tag{18}$$

is an array of δ-like functions centered on the $\vec{g}_s$ superlattice nodes. The number of superlattice nodes within the BZ is equal to ξ^{-1}. Since $I(\vec{Q}) = N(D^+)$ whenever $\vec{Q} = \vec{g}_s$, and $I(\vec{Q}) = 0$ otherwise, the sum rule gives

$$\sum_{\vec{Q}}^{\mathrm{BZ}} I(\vec{Q}) = \frac{N(D^+)}{\xi} = N, \tag{19}$$

as expected.

When comparing case (i) and case (ii), we first have to point out that Bragg scattering does not really limit the electron mobility. Thus, in case (i) the relaxation time will be limited only by the "von Laue" diffuse term, whereas it will be infinite in case (ii).

The comparison between the interference functions Eqs. (13), (14), and (18), of cases (i) and (ii), respectively, also gives a suggestion for an empirical picture of intermediate cases. A partially ordered charged center distribution will be tentatively described as a virtual superlattice arrangement of the D^+, with a given amount of disorder superimposed. Thus, a general interference function will be assumed as being an array of Gaussian shaped functions, having common dispersion σ, centered on the $\vec{g}_s$ reciprocal nodes of the virtual superlattice:

$$I(\vec{Q}) = A \sum_{\vec{g}_s} \exp\left(-\frac{\mid \vec{Q} - \vec{g}_s \mid^2}{\sigma^2} \right). \tag{20}$$

Here, the preexponential factor A must be determined in order for $I(\vec{Q})$ to satisfy the sum rule Eq. (10). We have (see the Appendix)

$$A = \frac{8\pi^3}{V}\frac{\xi N}{\sigma^3\pi^{3/2}\,\mathrm{erf}^3(L/\sigma)}, \tag{21}$$

where V is the volume of the crystal and L is the side of the cube whose volume is equal to the Ω_{BZ} one of the Brillouin zone. In the Appendix it is also shown that the $I(\vec{Q})$ given by Eqs. (20), (21) reduces to the one given by Eq. (13) [case(i)], or by Eq. (18) [case (ii)] in the two opposite cases of large or vanishing σ, respectively.

Finally, we will consider how the interference function given by Eq. (8) can be reduced to the $S_{++}(Q)$ structure factor of Refs. 4, 7, 8, and 13. Equation (8) gives

$$\begin{aligned} I(\vec{Q}) &= 1 + \xi\sum_{\vec{\rho}\neq 0}\left(\frac{\epsilon(\vec{\rho})}{\xi^2} - 1\right)e^{i\vec{Q}\cdot\vec{\rho}} + \xi\sum_{\vec{\rho}\neq 0} e^{i\vec{Q}\cdot\vec{\rho}} \\ &= (1-\xi) + \xi\sum_{\vec{\rho}\neq 0}(g_{++}-1)\,e^{i\vec{Q}\cdot\vec{\rho}} + \xi\sum_{\vec{\rho}\neq 0} e^{i\vec{Q}\cdot\vec{\rho}}. \end{aligned} \tag{22}$$

Here the pair correlation function $g_{++}(\vec{\rho})/\xi^2$ $(\vec{\rho}\neq 0)$ has been introduced. In Eq. (22) the first term is responsible for the diffuse scattering by an array of ξN scattering centers randomly distributed at the N lattice points, whereas the last terms gives Bragg scattering by a virtual crystal of centers of reduced scattering amplitude $\xi f_i(\vec{Q})$. The second term represents the contribution (positive or negative) of any type of order in the distribution of centers over the lattice sites; if long range order is absent, $\epsilon(\vec{\rho})$ can be replaced by ξ^2, and $g_{++}(\vec{\rho})$ by unity, when ρ is large. Using the continuous variable $\vec{r}$ instead of $\vec{\rho}$ we get, apart from Bragg scattering,

$$I(\vec{Q}) = (1-\xi) + n(D^+)\int[g_{++}(r)-1]\exp(i\vec{Q}\cdot\vec{r})d\vec{r}. \tag{23}$$

Here $n(D^+) = N(D^+)/V$ is the density of ionized D^+ donors. The function $g_{++}(\vec{\rho})$ must now vanish for vanishing r. For an isotropic distribution, which may be justified when long range is absent, Eq. (23) reduces to

$$I(Q) = (1-\xi) + \frac{4\pi}{Q}n(D^+)\int[g_{++}(r)-1]r\,\sin(Qr)dr. \tag{24}$$

When $\xi \ll 1$, as in practical cases, Eq. (24) coincides with the $S_{++}(\vec{Q})$ structure factor of Refs. 4, 7, 8, and 13.

III. POSITIVELY AND NEGATIVELY CHARGED CENTERS

Let us now consider the possibility of positively and negatively charged impurities being present together. In an n-type semiconductor, negatively charged impurities are the A^- compensating acceptors and, possibly, D^- donors having negative U Hubbard correlation energy. A well known example of this last case is the conjectural DX^- charge state of donor impurities in many III-V semiconductors.

In diamondlike structures positively and negatively charged impurities occupy different sites in the primitive cell. For example, in Si-doped (AlGa)As, owing to the amphoteric behavior of Si, D^+, and A^- occupy III and V group atom sites, respectively, whereas DX^- is believed to be displaced into a threefold coordinated interstitial site.[17] These complications will be neglected here by assuming the spatial configuration of the scattering centers to be described by a set of variables $\xi(\vec{l})$ so that $\xi(\vec{l}) = 1$ if a D^+ is present within the $\vec{l}$th primitive cell, $\xi(\vec{l}) = -1$ if a A^- or a DX^- is present, and $\xi(\vec{l}) = 0$ in all other cases. The scattering potential is then again given by Eq. (1) if now $U_i(\vec{r}-\vec{l})$ means the potential due to an isolated positively charged impurity in $\vec{l}$. Consequently, Eq. (3) is still valid and the interference function $I(\vec{Q})$ is still given by Eq. (8), provided that ξ is replaced by $(\xi_+ + \xi_-)$, where

$$\xi_+ = \frac{N(D^+)}{N}, \qquad \xi_- = \frac{N(A^-)+N(DX^-)}{N}. \tag{25}$$

The correlation parameters $\epsilon(\vec{\rho})$ may now be negative when lattice sites separated by $\vec{\rho}$ have a high probability of being occupied by impurities with opposite charges. In any case, $|\,\epsilon(\vec{\rho})\,|$ gives the probability that pairs separated by $\vec{\rho}$ are both occupied by charged centers regardless of their signs. More specifically, $\epsilon(\vec{\rho})$ can be written as

$$\epsilon(\vec{\rho}) = P_{++}(\vec{\rho}) + P_{--}(\vec{\rho}) - 2P_{+-}(\vec{\rho}), \tag{26}$$

where $P_{++}(\vec{\rho})$, $P_{--}(\vec{\rho})$, and $P_{+-}(\vec{\rho})$ are the probabilities that lattice sites separated by $\vec{\rho}$ are both occupied by pairs of positive, negative, or opposite charges, respectively. $I(\vec{Q})$ is then

$$\begin{aligned} I(\vec{Q}) = 1 &+ (\xi_+ + \xi_-)^{-1} \\ &\times \sum_{\vec{\rho}\neq 0}[P_{++}(\vec{\rho}) + P_{--}(\vec{\rho}) - 2P_{+-}(\vec{\rho})]\exp(i\vec{Q}\cdot\vec{\rho}). \end{aligned} \tag{27}$$

Let us now examine particular cases. For a random distribution of scattering centers [case (i)], a straightforward analysis gives

$$I(\vec{Q}) = (\xi_+ + \xi_-)^{-1}[\xi_+(1-\xi_+) + \xi_-(1-\xi_-) + 2\xi_+\xi_-]. \tag{28}$$

The interference function is independent of $\vec{Q}$ and it can be readily approximated to $I(\vec{Q}) = 1$, when $\xi_+ \ll 1$, $\xi_- \ll 1$, as for the cases in point. In the opposite case, of centers arranged in a superlattice [case (ii)], only Bragg scattering contributes to $I(\vec{Q})$, similarly to Eq. (18). The superlattice may be defined as having $N(A^-)+N(DX^-)$ unit cells, each of them containing a negatively charged center together with $p = N(D^+)/[N(A^-)+N(DX^-)]$ positive centers ordered within the cell itself. The interference function will be an array of δ functions centered on the ξ_-^{-1} superlattice nodes within the BZ. Intermediate cases between random and superlattice distributions could be tentatively described by substituting δ functions

with Gaussian shaped functions of common dispersion σ to account for disorder in the negative center distribution. A better description should also account for the distribution of the p positively charged centers within each cell, thus introducing one more parameter of order, at least, besides σ. Contrary to the case examined in Sec. II, the use of an interference function with the unique parameter σ may now result in too rough an approximation for the analysis of experimental mobility data. A further difficulty is related to ambiguities in defining the virtual superlattice. In fact, the number of unit cells could alternatively be assumed to be equal either to the number of positively charged centers or to the net difference $N(D^+) - [N(A^-) + N(DX^-)]$.

Finally, the interference function Eq. (27) can be written in a more convenient form by introducing correlation functions defined as ($\rho \neq 0$)

$$g_{++}(\vec{\rho}) = \frac{P_{++}(\vec{\rho})}{\xi_+^2}, \quad g_{--}(\vec{\rho}) = \frac{P_{--}(\vec{\rho})}{\xi_-^2},$$

$$g_{+-}(\vec{\rho}) = \frac{P_{+-}(\vec{\rho})}{\xi_+\xi_-}. \tag{29}$$

A straightforward analysis then gives

$$\begin{aligned} I(\vec{Q}) = {} & \frac{\xi_+(1-\xi_+) + \xi_-(1-\xi_-) + 2\xi_+\xi_-}{\xi_+ + \xi_-} + \frac{(\xi_+ - \xi_-)^2}{\xi_+ + \xi_-} \sum_{\vec{\rho}} \exp(i\vec{Q}\cdot\vec{\rho}) \\ & + \frac{\xi_+^2}{\xi_+ + \xi_-} \sum_{\vec{\rho}\neq 0} [g_{++}(\vec{\rho}) - 1] \exp(i\vec{Q}\cdot\vec{\rho}) + \frac{\xi_-^2}{\xi_+ + \xi_-} \sum_{\vec{\rho}\neq 0} (g_{--}(\vec{\rho}) - 1) \exp(i\vec{Q}\cdot\vec{\rho}) \\ & - \frac{2\xi_+\xi_-}{\xi_+ + \xi_-} \sum_{\vec{\rho}\neq 0} [g_{+-}(\vec{\rho}) - 1] \exp(i\vec{Q}\cdot\vec{\rho}). \end{aligned} \tag{30}$$

The first term represents the contribution of a disordered distribution of charges and the second one gives Bragg scattering by a virtual lattice of impurities having scattering amplitude $(\xi_+ - \xi_-) f_i(\vec{Q})$. When replacing $\vec{\rho}$ by the continuous variable $\vec{r}$ and assuming isotropic distributions, the interference function $I(\vec{Q})$ gives(ξ_+, $\xi_- \ll 1$),

$$\begin{aligned} I(\vec{Q}) = {} & 1 + \frac{4\pi}{Q} \frac{n_+^2}{n_+ + n_-} \int_0^\infty [g_{++}(r) - 1]\, r \sin(Qr) dr \\ & + \frac{4\pi}{Q} \frac{n_-^2}{n_+ + n_-} \int_0^\infty [g_{--}(r) - 1]\, r \sin(Qr) dr \\ & - \frac{4\pi}{Q} \frac{2n_+n_-}{n_+ + n_-} \int_0^\infty [g_{+-}(r) - 1]\, r \sin(Qr) dr. \end{aligned} \tag{31}$$

Here Bragg scattering has been excluded and n_+ and n_- are the total densities of positively and negatively charged scattering centers, respectively. Again the pair correlation functions g_{++}, g_{--}, and g_{+-} are assumed to vanish for $r \to 0$. Equation (31) coincides with the $S(Q)$ structure factor of Ref. 13.

IV. ANALYSIS OF EXPERIMENTAL MOBILITY DATA

In this section we give an example of the use of the interference function in the analysis of experimental mobility data in which spatial correlation effects are significant. We considered Hall effect data taken in Si-doped $Al_{0.25}Ga_{0.75}As$ samples, whose electrical properties are controlled by DX centers. The uncompensated donor density $N_d - N_a$ was 2×10^{18} cm^{-3}. Different sets of μ mobility data as a function of the n free electron concentration were here analyzed. In particular, μ and n were obtained as a function of time during isothermal capture transients in the temperaure range 110 – 140 K, starting from a $t = 0$ electron density reached by illuminating the sample with the same light-emitting diode light intensity. By eliminating time, $\mu = \mu(n)$ curves were obtained; two of them, corresponding to the extreme temperatures of 110 (curve 1) and 140 K (curve 2) are here considered (Fig. 1). In Ref. 11 these curves were analyzed by fitting each mobility value through an empirical N_{eff} effective density of isolated scattering centers. Spatial correlation effects were then particularly evident both for high n values in the $T = 110$ K curve and for low n values in the

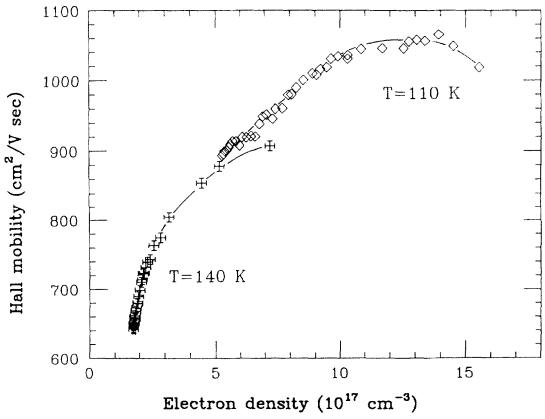

FIG. 1. Hall electron mobility vs free electron density during isothermal capture processes in $Al_{0.25}Ga_{0.75}As$ ($N_d - N_a \approx 10^{18}$ cm^{-3}) taken at $T = 110$ K (curve 1) and $T = 140$ K (curve 2). The data are taken from Ref. 11.

$T = 140$ K one. In fact, in the first case, corresponding to the initial stage of the capture process, the order in the charged center distribution appeared to increase as n decreased (decreasing N_{eff}), whereas, in the second case, the final stage of the capture process seemed to take place together with a disordering of the charge arrangement (increasing N_{eff}).

A steady-state $\mu = \mu(n)$ curve (curve 3) was also obtained at a lower temperature ($T = 7$ K) by varying n between the dark value n_{dark} and the one corresponding to the saturated photoconductivity condition (SPPC), n_{SPPC}. Each point of this curve was taken after the following thermal cycle:[11] lighting the sample at $T = 7$ K to saturate the persistent photoconductivity; heating the sample until activation of the capture process reduced the free electron density, rapid recooling of the sample to 7 K and taking the steady-state Hall measurement. These data are indicated in Fig. 2 with full circles. The mobility values measured through this experimental procedure are higher than those obtained for the same n after step by step illumination of the sample at $T = 7$ K, starting from the dark (open circles). These differences were attributed to the reaching of a higher order into the spatial distribution of the charged centers when n is varied passing through a capture process, instead of a random photoionization of the *DX* centers. We emphasize that an analogy exists between the behavior of curves 1 and 3 for high electron density and between curves 2 and 3 for low electron density. In fact, in curve 3, free electron densities just below n_{SPPC} were obtained by activating the electron capture into *DX* centers for a short time during the thermal cycle and then stopping the capture during the first stage of the process. On the other hand, low electron densities were reached after activation of the capture for a long time, in this case reaching the final stage of the process.

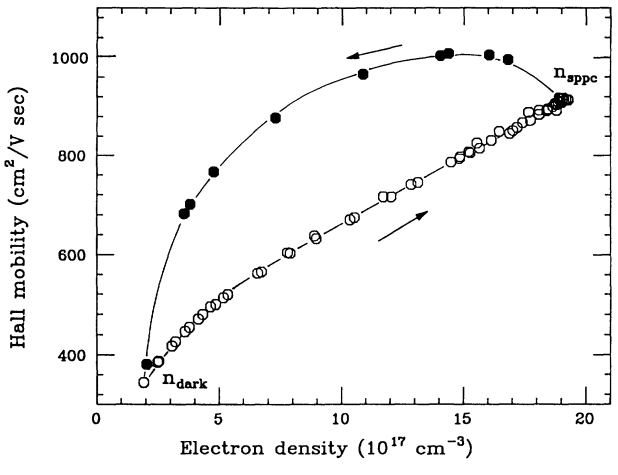

FIG. 2. Hall electron mobility vs free electron density at $T = 7$ K in $Al_{0.25}Ga_{0.75}As$ ($N_d - N_a \approx 10^{18}$ cm^{-3}). The lower curve (open circles) is obtained through subsequent photoionization steps (increasing n). In the higher curve (full circles) a given n is reached through capture processes during a proper thermal cycle starting from $n = n_{\text{SPPC}}$ (decreasing n), as explained in the text (curve 3). The data are taken from Ref. 11.

All the $\mu = \mu(n)$ curves 1 to 3 were here analyzed using the simplified form Eqs. (20), (21) of the interference function, as follows. The mobility was calculated within the relaxation time approximation, by taking into account the Fermi-Dirac statistics for a degenerate electron gas.[18] Two scattering mechanisms were considered, alloy scattering and ionized impurity scattering, so that the total momentum relaxation time is given by

$$\frac{1}{\tau(E)} = \frac{1}{\tau_i(E)} + \frac{1}{\tau_{\text{alloy}}(E)}. \tag{32}$$

An alloy scattering potential $V_{\text{al}} = 1.08$ was assumed, as suggested in Ref. 16, to evaluate $\tau_{\text{alloy}}(E)$, whereas the energy dependent relaxation time τ_i for impurity scattering was calculated for N_s screened isolated charged impurity per unit volume from

$$\frac{1}{\tau_i(k)} = \frac{N_s\, e^4\, m}{4\pi\, \hbar^3\, \epsilon^2\, k^3} \int_0^{2k} dQ\, \frac{Q^3}{(Q^2+\beta^2)^2}\, I(Q), \tag{33}$$

where $k = \sqrt{(2mE)}/\hbar$ and Q are the moduli of the incident electron wave vector and of the scattering vector, respectively; ϵ is the dielectric constant, m the electron effective mass, and β the screening parameter; e and $\hbar$ are the electron charge and the reduced Planck constant. An isotropic $I(Q)$ scattering function, as defined below, is used in Eq. (33).

The analysis was first performed according to the $U > 0$ model. Acceptors were considered only to evaluate the N_s charged impurity density as $N_s = n + 2N_a$, where a $N_a = 1.21 \times 10^{18}$ cm^{-3} acceptor density was used as obtained in Ref. 16 from data relative to the same sample. The number of unit cells per unit volume in the virtual superlattice was assumed as being equal to the difference $n(D^+) - N_a = n$, so that the $N(g_s)$ number of superlattice reciprocal nodes within the BZ was $N(g_s) = 4n^{-1}a^{-3}$, where a is the lattice parameter. After that, acceptors were neglected. The interference function Eqs. (20), (21), given as an array of Gaussian shaped functions with common dispersion σ, centered on the virtual superlattice reciprocal nodes, was assumed. The unique empirical parameter of order σ was then varied to fit each experimental mobility value. In this way the analysis was considerably simplified and rendered similar to the one for the case when all the centers have the same charge.

As to the details of the calculation, a simple cubic reciprocal superlattice cell was considered and its side taken as $g_o = [32\pi^3 a^{-3}/N(g_s)]^{1/3} = 2\pi n^{1/3}$, so that each reciprocal superlattice vector has modulus $g_s = g_o\sqrt{(i^2+j^2+l^2)}$, for integer values of i, j, and l. We have then to consider that the experimental mobility is a scalar quantity, independent of the orientation of the electric field. In order to account for this a mean on the solid angle was introduced in Eq. (20) by making any angle between $\vec{Q}$ and the $\vec{g}_s$ reciprocal superlattice vectors equally probable. This leads to an isotropic $I(Q)$ interference function and then to a $\tau_i(k)$ relaxation time independent of the direction of $\vec{k}$. This may be regarded

as a not too crude approximation if one considers that τ_i^{-1} is vanishing in the limit case when $I(\vec{Q})$ reduces to the anisotropic array of δ functions; on the contrary, τ_i^{-1} becomes larger and larger, increasing towards the limit value for a random distribution of charges, the more $I(\vec{Q})$ approaches an isotropic shape due to the increasing overlapping of neighboring Gaussian functions. The isotropic $I(Q)$ interference function is then

$$I(Q) = \frac{8\pi^3}{V}\frac{N}{\sigma^3\pi^{3/2}N(g_s)\ \mathrm{erf}^3(L/\sigma)} \times \sum_{\vec{g}_s}\left[\frac{1}{4\pi}\int d\Omega \exp\left(-\frac{|\vec{Q}-\vec{g}_s|^2}{\sigma^2}\right)\right] \quad (34)$$

that is, for $Q \neq 0$

$$I(Q) = \frac{8\pi^3}{V}\frac{N}{\sigma^3\pi^{3/2}N(g_s)\ \mathrm{erf}^3(L/\sigma)} \times \left(e^{-Q^2/\sigma^2} + \sum_{g_s\neq 0}\frac{\sigma^2}{4Qg_s}\left(e^{-(Q-g_s)^2/\sigma^2} - e^{-(Q+g_s)^2/\sigma^2}\right)\right). \quad (35)$$

The sum on g_s, which becomes a sum on i, j, and l, was extended to the whole BZ, but practically, for $\sigma < 10^7\ \mathrm{cm}^{-1}$, appreciable contributions were found only by $g_s < (10-15)g_o$.

The evaluated values of the ratio σ/g_o between the common dispersion σ and the g_o side of the virtual superlattice are reported in Fig. 3 (continuous lines) as a function of the free electron density for the 110 K and 140 K isothermal capture transients. The corresponding values of the N_{eff} effective density of isolated scattering centers, as evaluated in Ref. 11 are also shown for comparison. N_{eff} is independent of the choice of $U > 0$ or $U < 0$ model for the DX center. During the first stage of the capture process a decrease in σ/g_o is observed as n decreases: this agrees with the expected ordering of the charges through a spatially selective capture into DX centers, which removes as much as possible local fluctuations in electrostatic potential. In the intermediate stage of the process the electron capture takes place without important modification of the σ/g_o ratio. The final stage is characterized by a reduction of order in the scattering center distribution. This latter behavior is not observed at $T = 110$ K, owing to the limited duration of the experiment (300 min),[11] since the capture process is very slow at this temperature. On the other hand, the final stage becomes observable at $T = 140$ K, the capture being sufficiently fast, whereas in this case the region of constant σ/g_o is probably compressed between the initial and final stages of the process, owing to the limited variation of n. The analysis of the steady-state mobility data of Fig. 2 (full circles) is reported in Fig. 4. Also in this case, the corresponding N_{eff} values are indicated in the inset. Owing to a more widely investigated range of n, the initial stage of decrease in σ/g_o, the intermediate one and the final stage of increase in σ/g_o are well evident in this case.

The dashed lines in Figs. 3 and 4 give the ratio σ/g_o vs n when the N_s density of scattering centers in Eq. (33) is taken as $N_s = N_d - N_a$, independent of n, as for the $U < 0$ approach for the DX center [N_d =donor density= $n(D^+)+n(DX^-)$]. The value $N_s = 4.33\times 10^{18}$ cm^{-3} was used, as derived from the analysis given in Ref. 16 for the same sample. g_o was taken as being equal to $2\pi n^{1/3}$, as for the $U > 0$ case, thus assuming that the density of the unit cell of the virtual superlattice is again equal to the difference $n(D^+)-[n(DX^-)+N_a]$ between the densities of positively and negatively charged impurities. As for the $U > 0$ case, using the interference function [Eqs. (20), (21)] in the simplified isotropic form [Eq. (35)], the single parameter σ was determined by fitting the experimental mobility data. The above simplifications, which are made to analyze the experi-

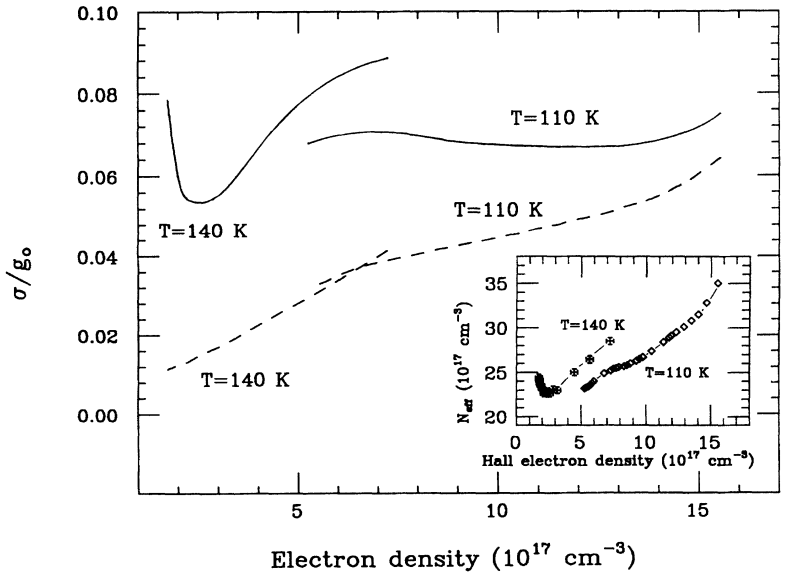

FIG. 3. Ratio σ/g_o as a function of the free electron density for the 110 K and 140 K isothermal capture transients; $U > 0$: continuous lines, $U < 0$: dashed lines. The corresponding values of the N_{eff} effective density of isolated scattering centers, as evaluated in Ref. 11, are reported in the inset for comparison.

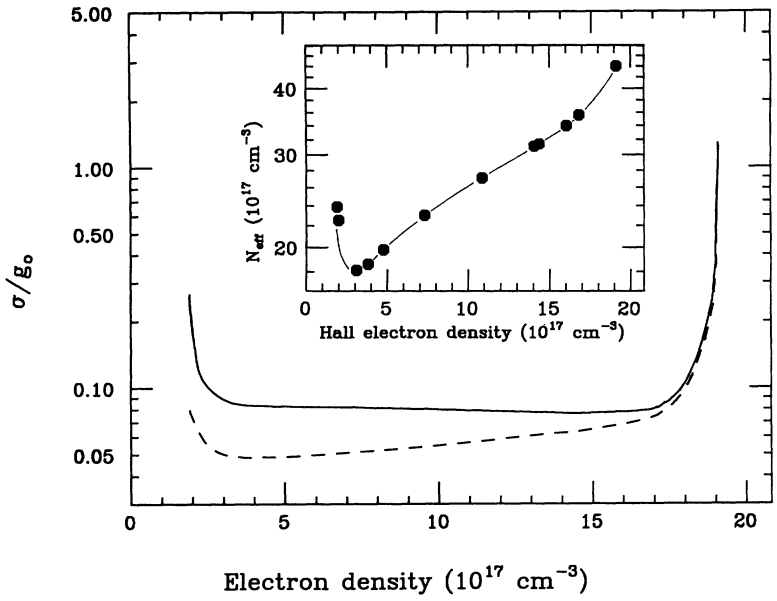

FIG. 4. Ratio σ/g_o as a function of the free electron density for the higher curve of Fig. 2 ($T = 7$ K); $U > 0$: continuous line; $U < 0$: dashed line. The inset gives the corresponding values of the N_{eff} effective density of isolated scattering centers, evaluated through the approach given in Ref. 11.

mental data in a way similar to the case of scattering centers with equal charges, are more easily justified in the positive U approach than in the negative U one. In fact, in the $U > 0$ case, complications are only due to acceptors: they are in a fixed position and can be reasonably neglected in scarcely compensated samples. In the $U < 0$ case, besides acceptors, DX^- charges have to be considered. For low values of n they are comparable in number to D^+; moreover their distribution may change owing to spatially selective capture processes. Our simplified $U < 0$ analysis is then expected to be less and less accurate the lower n becomes.

In spite of the above difficulties, the σ/g_o vs n curves obtained using positive or negative U approach have some important common features, especially in the analysis of steady-state mobility data, as can be seen in Fig. 4. The most important difference appears at low values of n, where the $U < 0$ analysis is rather inadequate to reveal the increasing disorder in the charge distribution which takes place at the final stage of the capture. In particular, the final increase in σ/g_o is lacking in the $U < 0$ analysis of the $T = 140$ K mobility transient (Fig. 3). This final disordering of the scattering centers is clearly suggested by the U-independent analysis which uses the empirical N_{eff} parameter (see the insets of Fig. 3 and 4). The absence of the σ/g_o final increase in Fig. 3, and the less evident one of Fig. 4 when compared with the $U > 0$ analysis, can then be interpreted as an indication that the simplifications we have made are too crude in the $U < 0$ case the lower n becomes.

Other common features are related to the order of magnitude of the ratio σ/g_o. In particular, as also discussed in Refs. 11 and 16, a random distribution of the scattering centers is expected under conditions of saturated persistent photoconductivity ($n = n_{\text{SPPC}}$), when all the donors are photoionized. Within this limit σ/g_o should tend to infinity, but practically every value above $\sigma/g_o \approx 1$ was found to give the experimental mobility. Regardless of the sign of U, values below $\sigma/g_s \approx 0.1$ were obtained during the intermediate stage of the capture process, when a partial order in the charge arrangement is reached: these small values indicate that a slightly disordered superlattice can be a satisfactory picture of the distribution. In other words, the capture takes place by realizing the maximum allowed distance between couples of neighboring charges, rendering the charged center distribution not too different from a regular lattice. This picture, which is alternative with respect to the ones based on local order parameters, seems to suggest that the local smoothing of the electrostatic potential fluctuations may have the global effect of introducing a rough long-range order in the distribution of charges. Although the absolute value of σ/g_o should not be considered too meaningful σ/g_o values near 0.1 mean that the scattering centers are displaced, on the average, from the sites of a regular superlattice of about 10% of the mean distance between neighboring centers. This latter is not far from 10^{-6} cm in the present situation. The increasing disorder which is observed in the final stage of the capture process is rather difficult to explain in terms of local fluctuations of the electrostatic potential. This is due to the exhaustion of free electrons before capture processes which increase significantly the total electrostatic energy beginning to take place. These are, for example, the formation of $DX^- - DX^-$ or $DX^- - A^-$ pairs ($U < 0$) or the transformation of $D^+ - A^-$ dipoles into $D^o - A^-$ pairs ($U > 0$). A tentative explanation could be more easily advanced in terms of a long-range order picture. We first have to consider that electron emission is a considerably less efficient process compared to capture. In fact, the activation energy for emission (0.44 eV, independent of x) is systematically larger than the x-dependent energy barrier for capture into DX centers.[1] The lower efficiency of the emission process is thus expected to prevent the rearrangement of the center distributions towards the one of maximum order allowed by the random distribution of the impurities. This limiting role of the emission should be more and more important as n diminishes, owing to

the increasing fraction of filled impurities.

Finally, we have to consider the question of how the above conclusions may depend on the particular choice of a simple cubic virtual superlattice. First, we have to point out that the density of unit supercells is determined by the charged impurity density alone. This latter being given, the g_o first neighbor distance between reciprocal superlattice nodes changes by only a factor near unity when different superlattices having cubic symmetry are considered. Moreover, the crucial parameter in fitting mobility values is the ratio σ/g_o rather than σ or g_o separately, as it can be argued by considering that σ/g_o determines the amount of overlapping between neighboring Gaussian shaped functions in $I(Q)$. All this suggests that the main features of the scattering center distribution resulting from the above analysis of mobility data are rather independent of the type of superlattice used in the picture. Anyway, although the details of the distribution of charges cannot be investigated through our analysis, a main result of this work is that the experimental $\mu = \mu(n)$ dependences can be fully described only if a given amount of long-range order is included in the distribution itself. This long-range order, which is due to selective capture processes during the initial stage of the capture, cannot fully survive at the final stage. As explained above, this may be understood by considering the role of low efficiency emission processes in limiting the redistribution of charges over the impurities.

V. CONCLUSIONS

Electron scattering by a spatially correlated system of charged centers has been described using the formalism of composition waves. The matrix element for the scattering rate is given through a $I(\vec{Q})$ ($\vec{Q}$ = scattering vector) interference function containing pair correlation parameters $\epsilon(\vec{\rho})$ defined at the $\vec{\rho}$ space lattice vectors. The $\epsilon(\vec{\rho})$ are able to describe long range as well as short range order. A comparison between the two extreme cases of randomly distributed scattering centers and of centers arranged in a superlattice suggest, for intermediate cases, a $I(\vec{Q})$ given by an array of Gaussian shaped functions with common dispersion σ, centered on the reciprocal nodes of a virtual superlattice. In the simple case of scattering centers with equal charges, the unique parameter σ can be used in fitting experimental mobility. A similar procedure can be tentatively carried out also when positively and negatively charged impurities are present together, although simplifications have to be made in this case. On this basis, experimental mobility data for Si-doped $Al_xGa_{(1-x)}As$ ($x = 0.25$) samples have been analyzed and discussed. Data refer to isothermal electron capture transients into DX centers, as well as to steady-state measurement taken for different values of the n free electron density under persistent photoconductivity regime. Both the cases of positive and negative U correlation energy for the DX center have been considered and discussed. The results of the analysis were given through the n dependence of the σ/g_o ratio, g_o being the size of the unit cell of the virtual superlattice in the reciprocal space. The $U > 0$ analysis confirmed that the initial stage of the capture takes place together with an increasing order in the scattering center distribution (decreasing σ/g_o), whereas a decreasing order (increasing σ/g_o) takes place in the final stage. The simplifications introduced in the $U < 0$ analysis seem to be inadequate only for revealing the final increasing disorder. Regardless of the U sign, the analysis has shown that values of σ/g_o as low as 0.1 or below are reached during the state of maximum order, thus confirming that a slightly disordered superlattice can be a satisfactory picture of the distribution of the scattering centers.

APPENDIX

The $I(\vec{Q})$ function Eq. (20) will satisfy the sum rule Eq. (10) if

$$A = \frac{8\pi^3 N}{V}\left[\sum_{\vec{g}_s}\int_{\mathrm{BZ}} d\vec{Q}\,\exp\left(-\frac{|\vec{Q}-\vec{g}_s|^2}{\sigma^2}\right)\right]^{-1}. \quad \text{(A1)}$$

When σ is much smaller than the g_o spacing between neighboring reciprocal superlattice nodes, the I integral of Eq. (A1) is equal to $\sigma^3\pi^{3/2}$, independent of $\vec{g}_s$. For nonspecific values of σ, a good approximation is to replace the sum over the ξ^{-1} reciprocal superlattice vector $\vec{g}_s$ with $\xi^{-1}\langle I\rangle$, where $\langle I\rangle$ is the mean value of I. By approximating the BZ with an equivalent cube of side L we have

$$\langle I\rangle = \sigma^3\pi^{3/2}\mathrm{erf}^3\left(\frac{L}{\sigma}\right), \quad \text{(A2)}$$

with

$$\mathrm{erf}(z) = \frac{2}{\sqrt{\pi}}\int_0^z dt\, e^{-t^2}. \quad \text{(A3)}$$

This leads to Eq. (21).

Let us now verify that the interference function reduces to Eq. (13) or (18) in the two opposite cases of large or vanishing σ, respectively. Consider first the case of large σ. Since $\xi \ll 1$ in the cases in point, the ξ^{-1} number of reciprocal superlattice nodes within the BZ is large, typically of the order of 10^4 for charged impurity concentrations in the 10^{18} cm^{-3} range. Then, if $\sigma \gg g_o$ we can make the approximation

$$\sum_{\vec{g}_s}\exp\left(-\frac{|\vec{Q}-\vec{g}_s|^2}{\sigma^2}\right) \approx \frac{\xi^{-1}}{\Omega_{\mathrm{BZ}}}\int d\vec{g}_s \exp\left(-\frac{|\vec{Q}-\vec{g}_s|^2}{\sigma^2}\right)$$
$$\approx \frac{\xi^{-1}}{N}\frac{V}{8\pi^3}\sigma^3\pi^{3/2}\mathrm{erf}^3\left(\frac{L}{\sigma}\right) = A^{-1}. \quad \text{(A4)}$$

From Eq. (20) we then get $I(\vec{Q}) \approx 1$ which clearly coincides with Eq. (13) for $\xi \ll 1$.

In the opposite case, of vanishing σ, each normalized Gaussian function in Eq. (20) reduces to a $\delta(\vec{Q} - \vec{g}_s)$ function centered on the corresponding $\vec{g}_s$ node

$$I(\vec{Q}) = \frac{8\pi^3}{V}\xi N \sum_{\vec{g}_s} \delta(\vec{Q} - \vec{g}_s). \quad \text{(A5)}$$

This satisfies the sum rule Eq. (10) since

$$\frac{V}{8\pi^3}\int_{\mathrm{BZ}} d\vec{Q}\; I(\vec{Q}) = \xi N \sum_{\vec{g}_s} \int d\vec{Q}\; \delta(\vec{Q} - \vec{g}_s)$$

$$= \xi N \xi^{-1} = N. \quad \text{(A6)}$$

Equation (A5) is then equivalent to the interference function given by Eq. (18).

[1] P. M. Mooney, J. Appl. Phys. **67**, R1 (1990).

[2] T. N. Theis, in *Proceedings Symposium on Defects in Materials, Boston, 1990*, edited by P. D. Bristowe, J. E. Epperson, J. E. Griffith, and Z. Liliental-Weber, MRS Symposia Proceedings No. 209 (Materials Research Society, Pittsburgh, 1991), pp. 367 and 368.

[3] E. P. O'Reilly, Appl. Phys. Lett. **55**, 1409 (1989).

[4] J. Kossut, Z. Wilamowski, T. Dietl, and K. Swiatek, in *Proceedings of the 20th International Conference on the Physics of Semiconductors, Thessaloniki, 1990*, edited by E. M. Anastassakis and J. D. Joannopoulos (World Scientific, Singapore, 1990), Vol. 1, p. 613.

[5] D. K. Maude, J. C. Portal, L. Dmowski, T. Foster, L. Eaves, M. Nathan, M. Heiblum, J. J. Harris, and R. B. Beall, Phys. Rev. Lett. **59**, 815 (1987).

[6] D. K. Maude, L. Eaves, T. J. Foster, and J. C. Portal, Phys. Rev. Lett. **62**, 1922 (1989).

[7] T. Suski, P. Wisniewski, E. Litwin-Staszewska, J. Kossut, Z. Wilamowski, T. Dietl, K. Swiatek, K. Ploog, and J. Knecht, Semicond. Sci. Technol. **5**, 261 (1990).

[8] Z. Wilamowski, J. Kossut, T. Suski, P. Wisniewski, and L. Dmowski, Semicond. Sci. Technol. **6**, B34 (1991).

[9] R. Piotrzkowski, L. Konczewicz, E. Litwin-Staszewska, J. L. Robert, and P. Lorenzini, Semicond. Sci. Technol. **6**, 250 (1991).

[10] W. Jantsch, G. Ostermayer, G. Brunthaler, G. Stoeger, J. Woeckinger, and Z. Wilamowski, in *Proceedings of the 20th International Conference on the Physics of Semiconductors, Thessaloniki, 1990*, edited by E. M. Anastassakis and J. D. Joannopoulos (World Scientific, Singapore, 1990), Vol. 1, p.485.

[11] P. L. Coz, C. Ghezzi, and A. Parisini, Semicond. Sci. Technol. **8**, 13 (1993).

[12] Z. Wilamowski, J. Kossut, W. Jantsch, and G. Ostermayer, Semicond. Sci. Technol. **6**, B38 (1991).

[13] P. J. van der Welt, M. J. Anders, L. J. Giling, and J. Kossut, Semicond. Sci. Technol. **8**, 211 (1993).

[14] M. A. Krivoglaz, *Theory of X-Ray and Thermal Neutron Scattering by Real Crystals* (Plenum Press, New York, 1969), Chaps. 1 and 5.

[15] A. G. Khachaturyan, Prog. Mater. Sci. **22**, 1 (1978).

[16] C. Ghezzi and A. Parisini, Semicond. Sci. Technol. **8**, 472 (1993).

[17] D. J. Chadi and K. J. Chang, Phys. Rev. B **39**, 10 063 (1989).

[18] A. Baraldi, C. Ghezzi, A. Parisini, A. Bosacchi, and S. Franchi, Phys. Rev. B **44**, 8713 (1991).